Type of contribution:
Editorial
▶ Research Paper
Case Study
Review Paper
Scientific Data
Report of Tech. Application

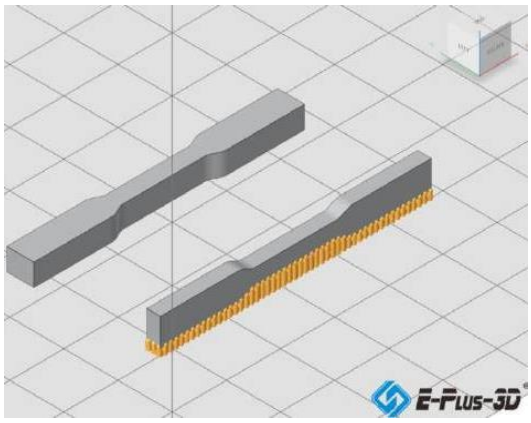
e-issn. 2798-5245

Mechanical Engineering for Society and Industry
Vol. 5, No. 2 (2025) pp 342-352
https://doi.org/10.31603/mesi.13238

Evaluation of dimensional accuracy on SLM product using 3D laser scanner

Moch. Agus Choiron[1]*, Anindito Purnowidodo[1], Achfas Zacoeb[2], Rosadila Febritasari[3], Willy Artha Wirawan[4], Imam Kusyairi[3], Johan Wayan Dika[3]

[1] Department of Mechanical Engineering, Universitas Brawijaya, Malang 65145, **Indonesia**
[2] Department of Civil Engineering, Universitas Brawijaya, Malang 65145, **Indonesia**
[3] Doctoral Program, Department of Mechanical Engineering, Universitas Brawijaya, Malang 65145, **Indonesia**
[4] Department of Mechanical Engineering, Universitas Negeri Surabaya, Surabaya 60231, **Indonesia**
✉ agus_choiron@ub.ac.id



Highlights:

- First-time evaluation of dimensional accuracy in SLM using 3D laser scanning technology.
- Compatibility between CAD models and SLM-printed products assessed via Geomagic Control X.
- Dimensional deviations found within ±0.1 mm tolerance range.
- Laser speed and print orientation identified as key factors influencing accuracy.

Abstract

Dimensional accuracy is a critical factor in additive manufacturing, especially in Selective Laser Melting (SLM). Recently, many studies had investigated the SLM process and products, but studies on the evaluation of SLM printing product to check the dimensional accuracy have not been explored. This study investigates the dimensional accuracy of SLM products by employing a 3D laser scanning technology and evaluate the compatibility between CAD designs and the final SLM printed products. The 3D laser scanning is performed using a high-precision 3D laser scanner, then continued by comparison with the CAD model through Geomagic Control X software. Dimensional accuracy was measured using visual and statistical parameters such as color graphic and deviation. Results showed that deviation of SLM printed products was within the tolerance range of ±0.1 mm. The main factors that affect accuracy are printing laser speed and print orientation. The 3D laser scanning technology proved to be effective for evaluating the dimensional accuracy of SLM printed products. This study contributes to develop the quality control methods in the field of metal-based additive manufacturing.

Keywords: Laser scanning; Additive manufacturing; Dimensional accuracy; Geomagic control; Selective Laser Melting (SLM)

Article info
Submitted: 2025-02-27
Revised: 2025-06-09
Accepted: 2025-06-22

This work is licensed under a Creative Commons Attribution-NonCommercial 4.0 International License

Publisher
Universitas Muhammadiyah Magelang

1. Introduction

Selective Laser Melting (SLM) is one of the additive manufacturing (AM) technique that offering the capability to fabricate complex geometries with high precision and functional properties [1], [2]. The mechanism of SLM technology involves a layer-by-layer additive manufacturing process that uses a high-energy laser to selectively fuse metallic powder particles [3]. This process allows SLM to fabricate intricate, high-precision components with excellent mechanical properties, making it suitable for critical applications in aerospace [4], biomedical implant [5], and automotive industries [6]. In the other side, the dimensional accuracy of SLM printed products is critical challenge due to inherent process-induced variations, such as scanning strategies [7], [8], [9]. The scanning strategy has effect in SLM process, such as laser power, scanning

speed, hatch spacing, and layer thickness [10], [11]. Ivan A. Pelevin *et al*. [12] suggested to set the scanning strategy based on the material so the final product can reach the product requirement especially reduced voids and cracks, and achieved relative densities above 95%. Meena Pant *et al.* examines the dimension precision of a product with flat and curve contour, and found that the sample length was slightly shorter than nominal values, but all measurements fell within acceptable error ranges [13]. From those problems, dimensional accuracy is a crucial parameter in SLM printed products, as it directly affects the functional performance, assembly tolerances, and overall printed product quality. To solve this, advanced metrology tools like 3D laser scanners have been increasingly utilized to evaluate and quantify dimensional deviations in AM products [14]. These scanners provide a non-contact inspection and high-precision of capturing the geometric features of complex components.

Several studies had investigated the dimensional accuracy in SLM processes or other fabricated process using non-contact inspection tools like 3D laser scanners or cameras. Yosef Wakjira *et al*. investigated the dimensional accuracy of 3D printed human femur bone models by combining reverse engineering (RE) and additive manufacturing (AM) technologies using three non-contact 3D laser scanners and found the mean deviation was approximately 0.46 mm [15]. Michael Kalms *et al*. proposed a quality control process using structured light-based metrology by utilizing the two cameras, which measures the dimensions of both the printed part and the powder deposition layer by layer [16]. The dimensional accuracy of thin-wall components that fabricated by Laser-Powder Bed Fusion was investigated by Josef Tomas *et al*. and found that the scan strategy was improved the dimensional accuracy [17]. Burak Yilmaz *et al*. conducted the deviation analysis of dental crowns using a metrology-grade software (Geomagic Control X) and a nonmetrology-grade 3D analysis software (Medit Link) and resulted that those assessment approaches were capable for evaluating the trueness of CAD and fabricated dental crown [18]. Cezarina Afteni *et al*. enhanced the quality control of machined part wih non-contact inspection by scanning the part then compared to the CAD model and proved that this technology is able to inspect the dimensional comprehensively [19]. Dong Wang *et al*. said that the traditional manual inspections are time consuming so they recommended the 3D laser scanner after they inspected the rebar spacing and length in prefabricated bridge components [20].

However, the utilization of 3D laser scanning technology for evaluating the dimension of SLM-produced parts remains underexplored. This study aims to fill the gap by applying a 3D laser scanner to assess the dimensional deviations of SLM-fabricated parts. The state of the art involves advanced non-contact inspection tools, like 3D laser scanners named Faro, then paired with Geomagic Design X dan Geomagic Control X, for evaluating the dimensional accuracy and minimizing the anaccuracy of measurement.

2. Materials and Methods

This study evaluated the dimensional accuracy of specimens fabricated by Selective Laser Melting (SLM). Flat tensile test specimens were designed according to ASTM E8 standards using CAD software and exported as STL files for printing. The specimens were produced using AlSi10Mg powder with three distinct printing strategies. Nine specimens were printed: three with a 90° orientation (specimen A) and six with a 0° orientation (specimen B and C), differing in bar support diameter and scanning parameters.

After printing process, the specimens were removed from the build platform, cleaned to eliminate residual powder, and scanned using a Faro Quantum Max 7-Axis laser scanner. The scanning process utilized non-contact laser projection to capture surface geometry. Scanned data were exported as STL files and aligned with CAD models using Geomagic Design X software. The sca nned data was cleanning it's unwanted area, filling gaps, and aligning multiple scans using best-fit alignment techniques. The cleaned data were converted into surface models and then solid CAD models. Dimensional deviations were evaluated by comparing the scanned STL files with reference CAD models, with deviations visualized using color maps and quantified against a 0.1 mm tolerance. This process ensured high accuracy in identifying inconsistencies between the fabricated specimens and their design.

3. Results and Discussions

The present study evaluated the dimensional accuracy of specimens produced through selective laser melting (SLM). The specimens were flat tensile testing that designed based on the

ASTM E8 standard, as shown in **Figure 1**. ASTM E8 tensile test specimens were modeled in CAD software then was exported as a Standard Tessellation Language (STL) file to be prepared as printing file. The specimens were fabricated from AlSi10Mg powder using SLM technology. The nine specimens were printed in different printing strategies that shown in **Table 1**.

Each strategy involves three specimens, with a total of nine produced for the study. Specimen A was printed with a 90° orientation relative to the X-axis. Specimen B and Specimen C were printed with a 0° orientation relative to the X-axis that can be seen in **Figure 2**. Specimens A and B used 1.5 mm bar supports, whereas Specimen C employed 2 mm. In the printing preparation process, variations in speed and power for volume support, part scanning, and bar support strategies were implemented to assess their impact on structural quality. Notably, specimen C featured slower support scanning, faster outer scanning, and distinct downskin border parameters. These printing strategies aimed to reduce the excessive heat accumulation during the printing process which can decrease the distortion [11].

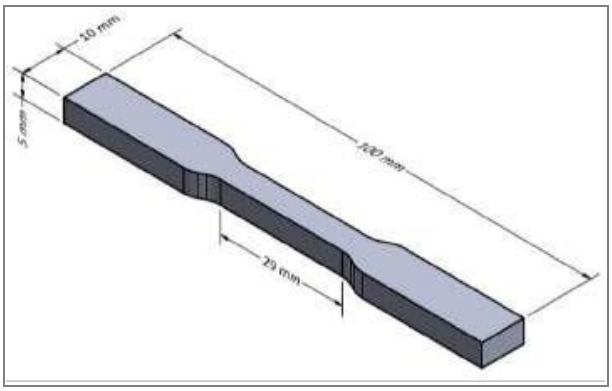


Figure 1. ASTM E8 tensile test specimen

After printing process, the specimens were on the platform that can be seen in **Figure 3** then cut and cleaned to remove loose powder. The specimens were scanned using 3D scanning tool with specification in **Table 2**. Scans were exported as STL files (test-scan STL) and imported into reverse engineering software using Geomagic Control X 2024. The STL files were aligned with the reference CAD model (CAD-Step) using a best-fit alignment method. Dimensional deviations were evaluated by comparing test-scan STL with CAD- Step. Measurements focused on key features such as thickness, length, and fillet radii of the specimens. Deviations were quantified as the maximum deviation with tolerance of 0,05 mm and the color map was generated for each specimen to visualize dimensional inconsistencies [18].

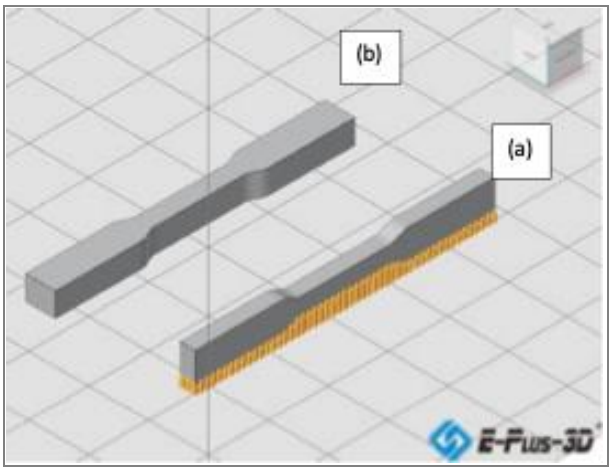


Figure 2. The orientation of printed specimens in: (a) 90° of X axis; (b) 0° of X axis

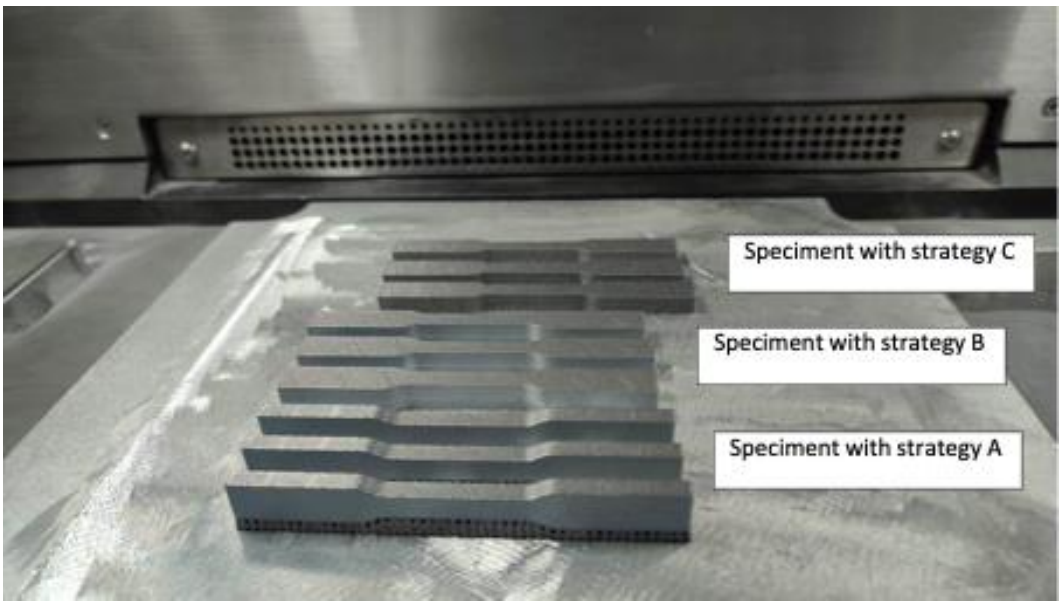


Figure 3. The 9 specimens after printing process

Table 1. The printing strategies of each speciments

	Strategy A	Strategy B	Strategy C
Number of speciments	3	3	3
Orientation	90° of X axis	0° of X axis	0° of X axis
Bar Support diameter	1.5 mm	1.5 mm	2 mm
Volume support dan part scan strategy:			
Support speed	2600 mm/s	2600 mm/s	1500 mm/s
Support power	200 W	200 W	180 W
Outer speed	300 mm/s	300 mm/s	400 mm/s
Outer power	270 W	270 W	240 W
Inskin speed	1000 mm/s	1000 mm/s	900 mm/s
Inskin power	370 W	370 W	240 W
Downskin speed	2000 mm/s	2000 mm/s	2400 mm/s
Downskin power	240 W	240 W	160 W
Downskin border speed	-	-	800 mm/s
Downskin border power	-	-	60 W
Bar support scan strategy:			
Support speed	2600 mm/s	2600 mm/s	0 mm/s
Support power	200 W	200 W	0
Inskin speed	1000 mm/s	1000 mm/s	1700 mm/s
Inskin power bar support	330 W	330 W	350 W
Outer speed	-	-	300 mm/s
Outer power	-	-	270 W
Downskin speed	-	-	2400 mm/s
Downskin power	-	-	240 W

Table 2. Specification of speciments

	Faro Quantum Max
Scanning method	Laser Line Probe
Axis	7
Max Scan Width (mm)	250
Mid Scan Width (mm)	185
Min Scan Width (mm)	120
Accuracy (µm)	25
Depth of field (mm)	205
Accompanying software	Geomagic Design X and Geomagic Control X
Max Point per Line	4000
Max scan rate	600 Hz
Point Acquistion rate	1.200.000 points per second
Laser type	450 nm/ 635 nm, Class 2

In this study, the scanning strategy employed by the Faro Quantum Max 7 Axis which is approached to Non-contact scanning. In the scanning process, this tool utilize advanced laser or light systems to collect data without physically interacting with the object. This method is particularly advantageous for scanning smooth surfaces materials with intricate details, as it eliminates the risk of damage or deformation on the surface part. The Faro scanner captures the data by projecting laser beams in a structured pattern, such as lines or points, across the object's surface, as illustrated in **Figure 4**. And the scanning angle can effect the consistency and accuracy of the resulting data. Yosef Wakjira *et al*. [15] declared that angles that align with optimal coherence between the laser beam or camera sensors and the surface can enhance precision, while unsuitable angles may cause deviations, such as shadowing or incomplete data capture. As the laser interacts with the surface geometry, the scanner's high-precision sensors capture the reflected light. To ensure consistent measurement accuracy when using a laser scanner manually in this study, the measurement process utilized the blue and red light as visual reference that can be seen in **Figure 4b**. These light beams are functioned as critical guidance for alignment and positioning during the scanning process. The blue and red lights create visible lines that help the operator align the scanner accurately with the object being measured. These light beams' intersection often indicates the optimal distance and orientation of the scanner relative to the object. These light beams also offer real-time feedback, enabling the operator to adjust the scanner's angle or distance dynamically, thereby maintaining consistency throughout the process. With a point acquisition rate of 1.2 million points per second, the Faro Quantum Max can quickly and efficiently gather detailed data. Its maximum scan rate of 600 Hz ensures fast scanning without compromising accuracy, as shown in **Figure 5**. Additionally, the scanner uses laser wavelengths of 450 nm/635 nm, Class 2, ensuring safe operation while maintaining high-resolution scanning. The reflected signals are then analyzed to construct an accurate representation of the surface.

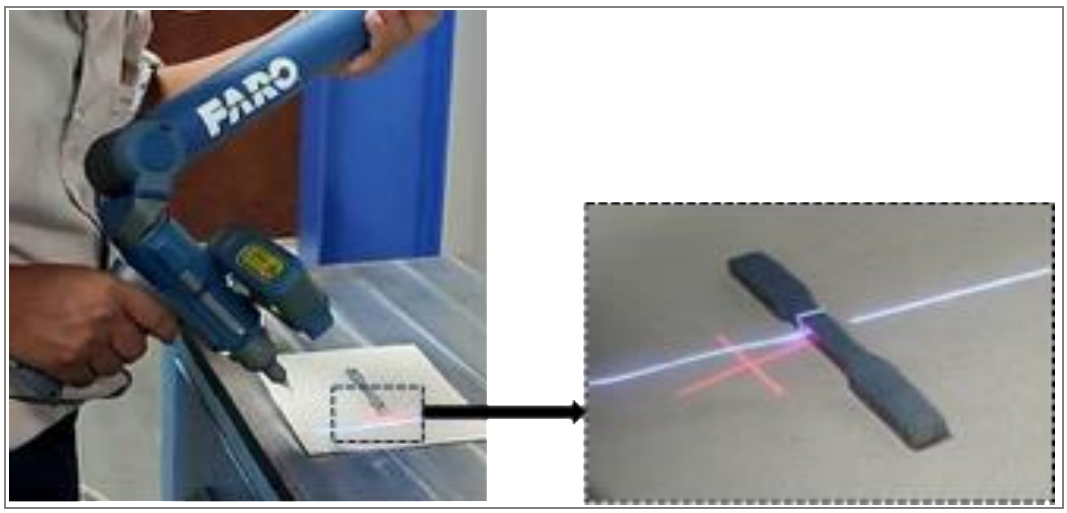


Figure 4. A suitable 3D scanning position for a speciment model

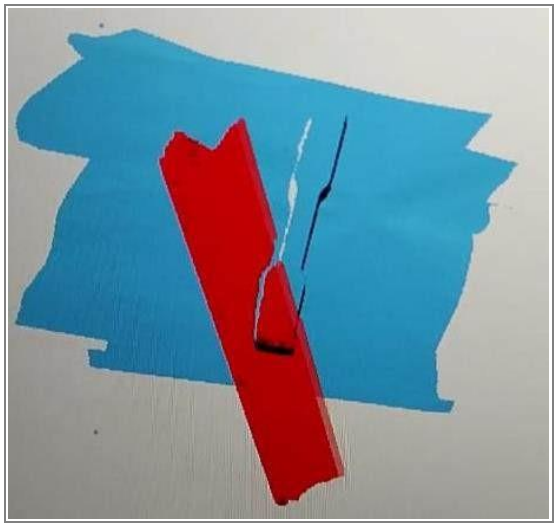


Figure 5. Illustration of scanning result

After the scanning process finished, the next step is post processing. Post-processing in Geomagic Design X involves several key steps, that can be seen in **Figure 6** to transform raw 3D scan data into an editable and accurate CAD model. Initially, scan data typically consists of point clouds or meshes. These data points represent the surface geometry of the scanned object, but they are often noisy, incomplete, or contain inaccuracies that need to be addressed. Then the scan data is imported and cleaned by removing noise and filling gaps. The noise appears due to surface imperfections, scanner errors, or environmental factors. So, there is tool to filter out these unwanted points then remove them in Geomagic Design X such as Noise Reduction Tool. This tool provides adjustable parameters, such as tolerance level and filter strength, which can be set to control the noise removal process. By carefully adjusting these settings, you can ensure that only extraneous data is eliminated while preserving the integrity of the original geometry. In this study, 0% measurement error impossible to be achived, but the software provides tools to minimize errors and improve accuracy significantly such as Noise Reduction Tool and we can also compare the processed data to the original CAD model using the Deviation Analysis tool. This comparison helps verify that the cleaned data remains accurate to the desired tolerances.

Sometimes, the scan data may have missing sections due to occlusions or limitations in the scanning process. The software provides features to fill these gaps using algorithms that estimate missing data based on neighboring points. After this, the alignment process should be conducted if multiple scans are taken. It can be done using automated or manual alignment techniques. This process combines these multiple scan datasets into a single unified model. Once the scan data has been cleaned and aligned, the next step is cleanning data that is then converted into a surface model. After the surface model is created, the next stage involves converting this surface into solid CAD model. After processing the scan data, the next step is to validate the model against the original scan data to ensure accuracy. Deviation analysis is conducted to compare the CAD model with the original scan data for accuracy in Geomagic Control X. Geomagic Control X provides tools to fit position between the final CAD model and the original scan data that is alignment tool. Saoirse O'Toole *et al*. investigated the limitations of various alignment algorithms used in defect measurement [21]. The result showed that the reference best-fit alignment tool can produce significantly lower alignment errors and more accurate measurements compared to standard best-fit and landmark-based alignment techniques. After the alignment process, deviation bar was generated in each location that want to be inspected, as shown in **Figure 7**. This deviation bar shows any differences between the model and the scan data. These differences are often displayed in color-coded maps, highlighting areas where the CAD model deviates from the scanned geometry as shown in **Figure 8** and **Figure 9**.

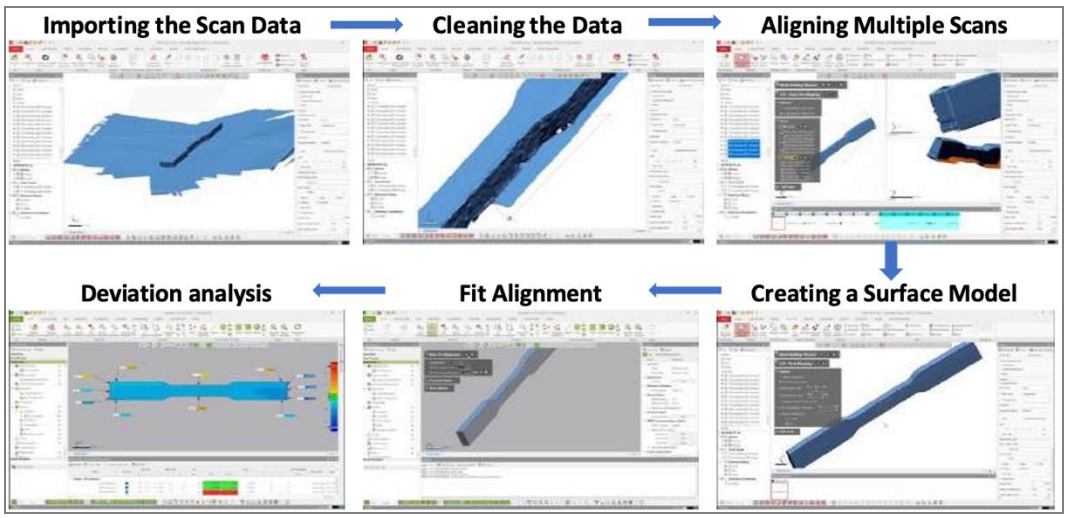


Figure 6. Illustration of post processing in Geomagic Design X and Geomagic Control X

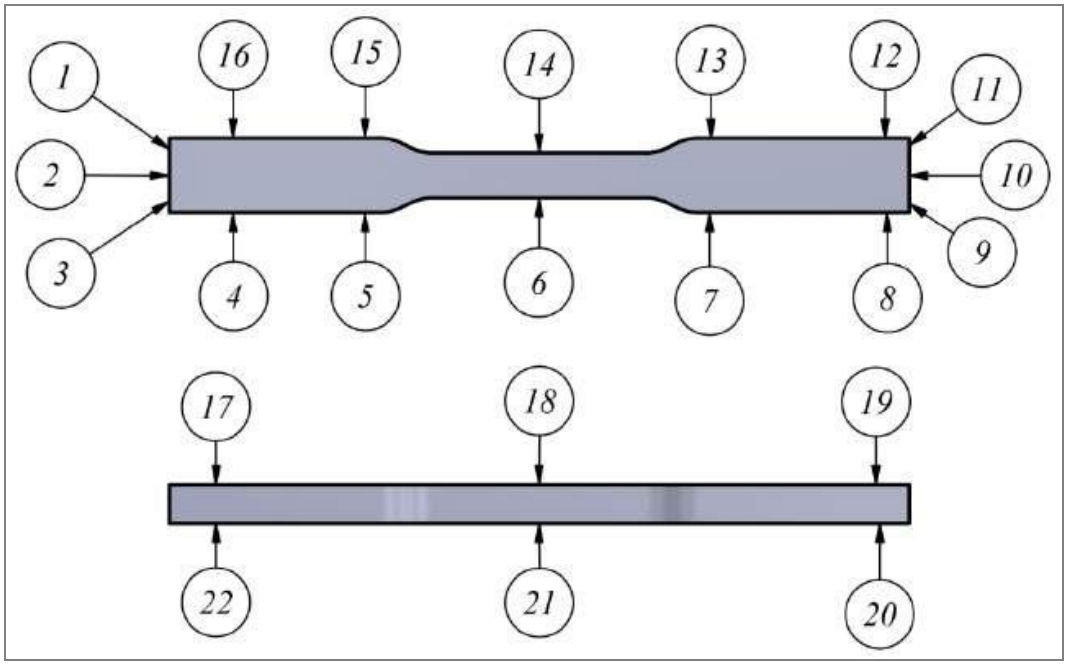


Figure 7. Deviation inspection points

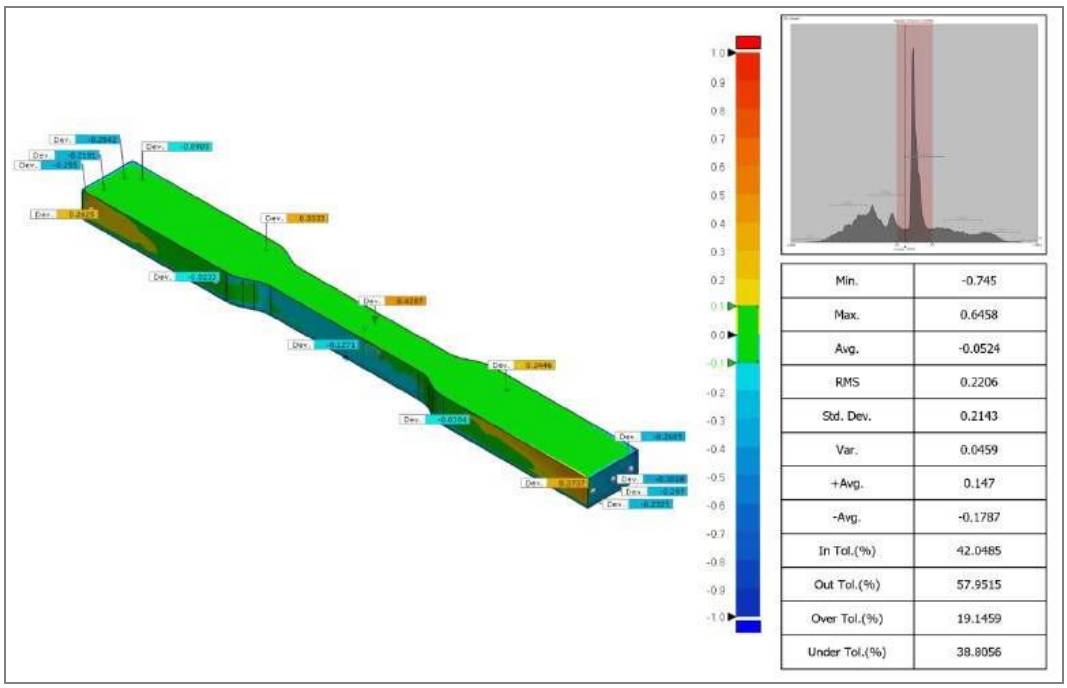
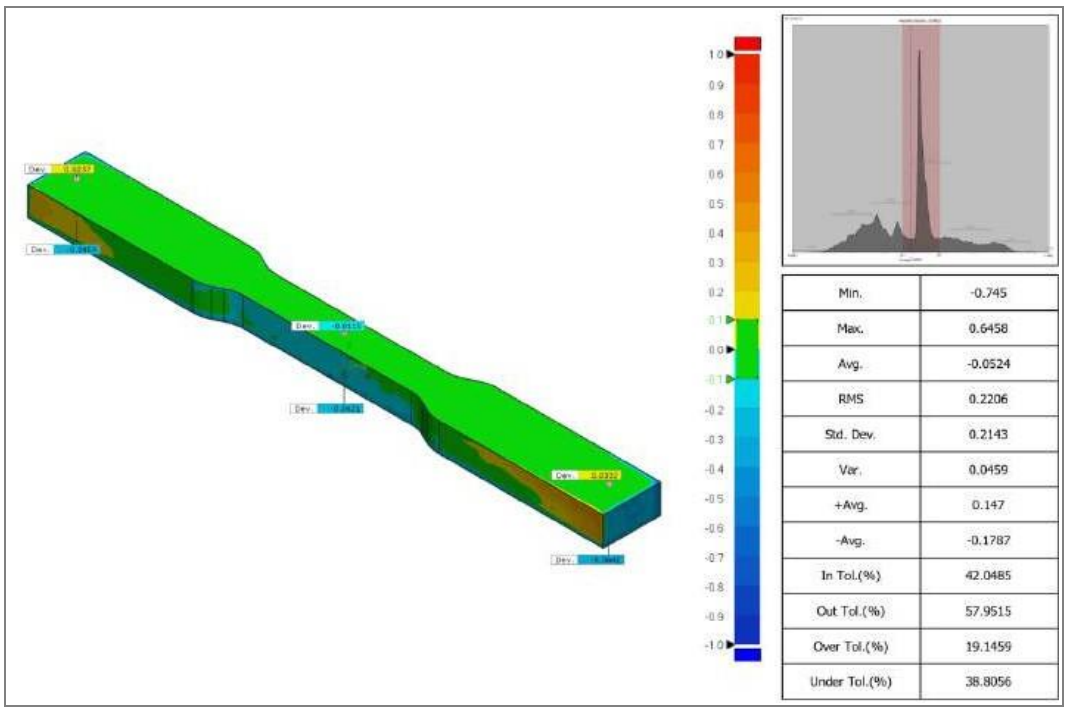


Figure 8. Deviation results in isometric view for 1st until 16th point



Min.	-0.745
Max.	0.6458
Avg.	-0.0524
RMS	0.2206
Std. Dev.	0.2143
Var.	0.0459
+Avg.	0.147
-Avg.	-0.1787
In Tol.(%)	42.0485
Out Tol.(%)	57.9515
Over Tol.(%)	19.1459
Under Tol.(%)	38.8056

Figure 9. Deviation results in isometric view for 17^{tt} until 22th point

As shown in **Appendix 1**, the data outlines the minimum and maximum deviations of specimens produced using three distinct fabrication strategies: A, B, and C. Strategy A consistently exhibits higher maximum deviations across all specimens compared to Strategy C, indicating less precise dimensional accuracy. However, these deviations are larger compared to Strategies B and C, indicating that the 90° orientation and bar support parameters used in this strategy may contribute to increased distortion.

In contrast, Strategy B shows the widest range of deviations among the three strategies, reflecting significant inconsistencies in fabrication accuracy. The inconsistency among specimens suggests that the 0° orientation and scanning parameters used in this strategy result in variable quality. Improvements in bar support diameter or scanning power could help address these variations and enhance dimensional accuracy.

Strategy C achieves the smallest and most consistent deviations, with minimum values as low as -0.0139 mm and maximum deviations generally not exceeding 0.2506 mm, that can be seen in **Figure 10**. This strategy demonstrates the highest level of precision, likely due to its optimized support and downskin parameters. Overall, Strategy C's performance highlights its potential as the most effective approach among the three strategies.

The color mapping results provide a clear visual representation of the dimensional deviations across the specimens for each strategy. For Strategy A, the mapping likely indicates widespread deviations across the geometry of the specimens, reflecting the relatively high and consistent deviation values observed in the data. For Strategy B, the color mapping is expected to show uneven patterns, consistent with the wide range of deviations observed. In contrast, the color mapping for Strategy C specimens would reveal more uniform color distributions, corresponding to the lower and more consistent deviations recorded.

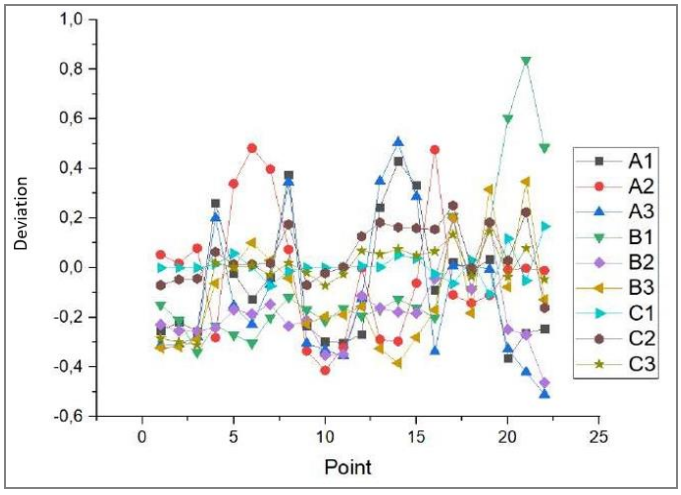


Figure 10. Graphic of deviation plotting

4. Conclusion

The conclusion of this study is the use of a 3D scanner proved to be highly effective and efficient for inspecting the dimensional accuracy of SLM-fabricated specimens. With its non-contact laser scanning technology, the 3D scanner provided precise and detailed measurements, capturing surface geometry. Additionally, the ability to visualize deviations through color mapping enhanced the identification of inconsistencies, making the 3D scanner an invaluable tool for quality control and process optimization in advanced manufacturing.

Acknowledgements

The authors gratefully acknowledge the use of the 3D Printing Metal Machine and 3D Laser Scanner at the Integrated Research Laboratory - Universitas Brawijaya (LRT-UB) for supporting this research. The facility provided invaluable resources and technical assistance that contributed significantly to the success of this study.

Authors' Declaration

Authors' contributions and responsibilities - The authors made substantial contributions to the conception and design of the study. The authors took responsibility for data analysis, interpretation and discussion of results. The authors read and approved the final manuscript.

Funding – Riset Pengembangan FT UB 2024.

Availability of data and materials - All data is available from the authors.

Competing interests - The authors declare no competing interests.

Additional information – No additional information from the authors.

References

[1] C. Zhang, D. Ouyang, S. Pauly, and L. Liu, "3D printing of bulk metallic glasses," *Materials Science and Engineering R: Reports*, vol. 145, no. June, p. 100625, 2021, doi: 10.1016/j.mser.2021.100625.

[2] M. Leary *et al.*, "Selective laser melting (SLM) of AlSi12Mg lattice structures," *Materials and Design*, vol. 98, pp. 344–357, 2016, doi: 10.1016/j.matdes.2016.02.127.

[3] H. R. Lashgari, M. Ferry, and S. Li, "Additive manufacturing of bulk metallic glasses: Fundamental principle, current/future developments and applications," *Journal of Materials Science and Technology*, vol. 119, pp. 131–149, 2022, doi: 10.1016/j.jmst.2021.09.068.

[4] R. Stolt and F. Elgh, "Introducing design for selective laser melting in aerospace industry," *Journal of Computational Design and Engineering*, vol. 7, no. 4, pp. 489–497, 2020, doi: 10.1093/jcde/qwaa042.

[5] A. N. Aufa *et al.*, "Current trends in additive manufacturing of selective laser melting for biomedical implant applications," *Journal of Materials Research and Technology*, vol. 31, no. May, pp. 213–243, 2024, doi: 10.1016/j.jmrt.2024.06.041.

[6] J. Piekło and A. Garbacz-Klempka, "Use of selective laser melting (SLM) as a replacement for pressure die casting technology for the production of automotive casting," *Archives of Foundry Engineering*, vol. 21, no. 2, pp. 9–16, 2021, doi: 10.24425/afe.2021.136092.

[7] D. Xie *et al.*, "A Review on Distortion and Residual Stress in Additive Manufacturing," *Chinese Journal of Mechanical Engineering: Additive Manufacturing Frontiers*, vol. 1, no. 3, p. 100039, 2022, doi: 10.1016/j.cjmeam.2022.100039.

[8] S. Chen, H. Gao, Y. Zhang, Q. Wu, Z. Gao, and X. Zhou, "Review on residual stresses in metal additive manufacturing: formation mechanisms, parameter dependencies, prediction and control approaches," *Journal of Materials Research and Technology*, vol. 17, pp. 2950–2974, 2022, doi: 10.1016/j.jmrt.2022.02.054.

[9] H. Jia, H. Sun, H. Wang, Y. Wu, and H. Wang, "Scanning strategy in selective laser melting (SLM): a review," *International Journal of Advanced Manufacturing Technology*, vol. 113, no. 9–10, pp. 2413–2435, 2021, doi: 10.1007/s00170-021-06810-3.

[10] A. Salmi, E. Atzeni, L. Iuliano, and M. Galati, "Experimental Analysis of Residual Stresses on AlSi10Mg Parts Produced by Means of Selective Laser Melting (SLM)," *Procedia CIRP*, vol. 62, pp. 458–463, 2017, doi: 10.1016/j.procir.2016.06.030.

[11] Y. Liu *et al.*, "An optimized scanning strategy to mitigate excessive heat accumulation caused by short scanning lines in laser powder bed fusion process," *Additive Manufacturing*, vol. 60, no. July, 2022, doi: 10.1016/j.addma.2022.103256.

[12] I. A. Pelevin *et al.*, "New Scanning Strategy Approach for Laser Powder Bed Fusion of Nd-Fe-B Hard Magnetic Material," *Metals*, vol. 13, no. 6, 2023, doi: 10.3390/met13061084.

[13] M. Pant, L. Nagdeve, G. C. Moona, and H. Kumar, "Dimensional accuracy and stability analysis of laser powder bed fusion (LPBF) samples: implications of process variables," *International Journal on Interactive Design and Manufacturing (IJIDeM)*, vol. 18, no. 3, 2023.

[14] R. Vrána *et al.*, "Deviations of the SLM Produced Lattice Structures and Their Influence on Mechanical Properties," 2022. doi: 10.3390/ma15093144.

[15] Y. Wakjira, N. S. Kurukkal, and H. G. Lemu, "Assessment of the accuracy of 3D printed medical models through reverse engineering," *Heliyon*, vol. 10, no. 11, p. e31829, 2024, doi: 10.1016/j.heliyon.2024.e31829.

[16] M. Kalms, R. Narita, C. Thomy, F. Vollertsen, and R. B. Bergmann, "New approach to evaluate 3D laser printed parts in powder bed fusion-based additive manufacturing in-line within closed space," *Additive Manufacturing*, vol. 26, no. January, pp. 161–165, 2019, doi: 10.1016/j.addma.2019.01.011.

[17] J. Tomas *et al.*, "The dimensional accuracy of thin-walled parts manufactured by laser-powder bed fusion process," *Journal of Manufacturing and Materials Processing*, vol. 4, no. 3, 2020, doi: 10.3390/JMMP4030091.

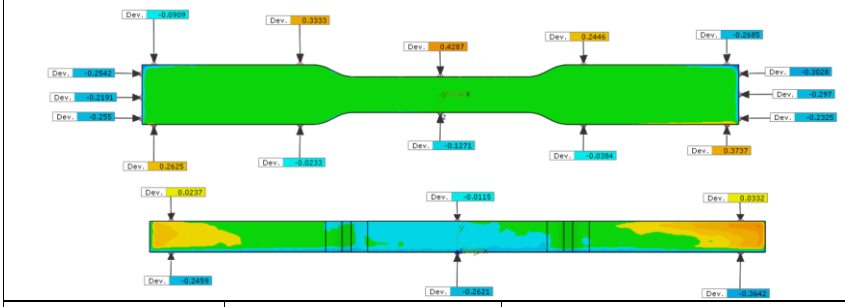
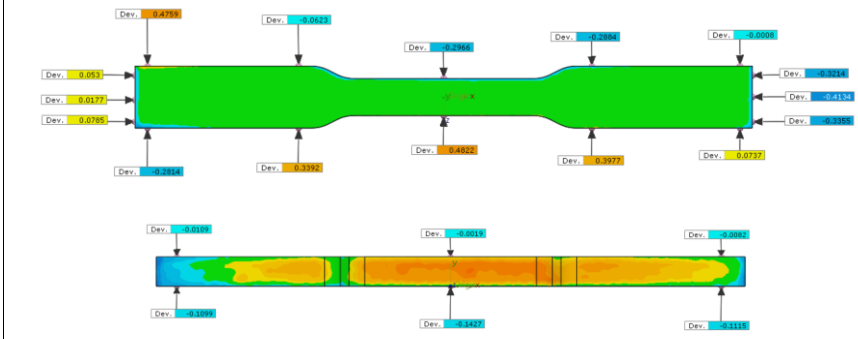
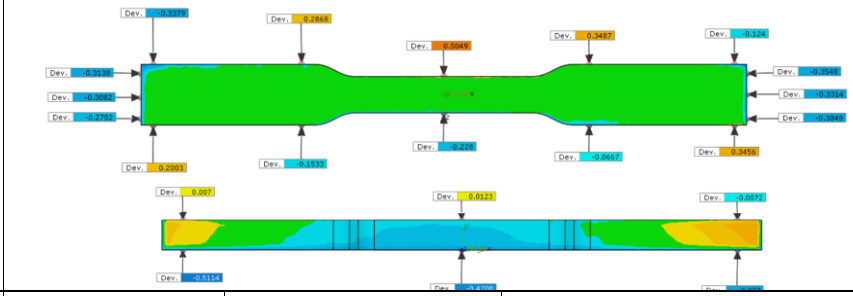
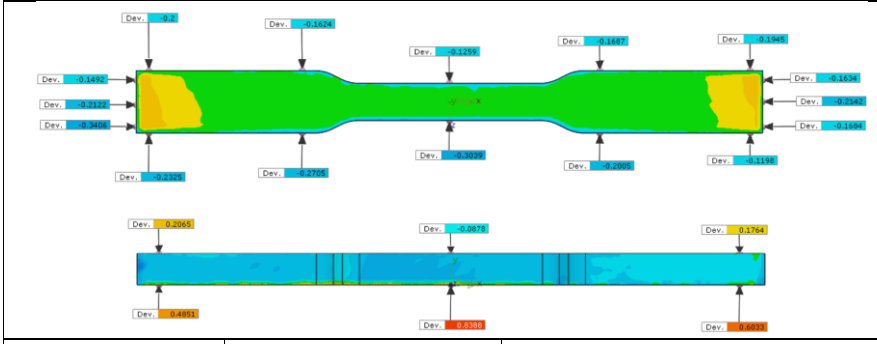
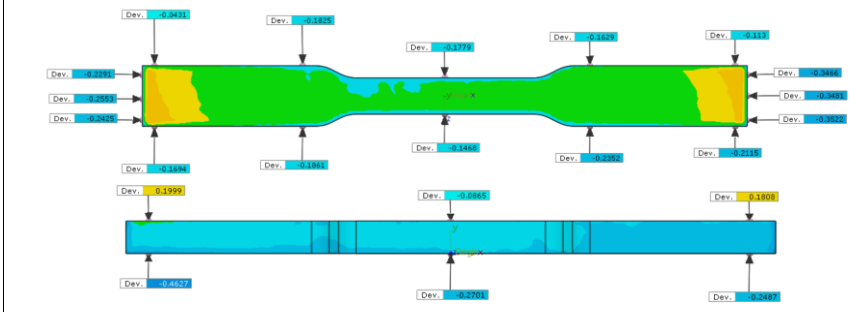
[18] B. Yilmaz *et al.*, "Influence of 3D analysis software on measured deviations of CAD-CAM resin crowns from virtual design file: An in-vitro study," *Journal of Dentistry*, vol. 118, no. October 2021, 2022, doi: 10.1016/j.jdent.2021.103933.

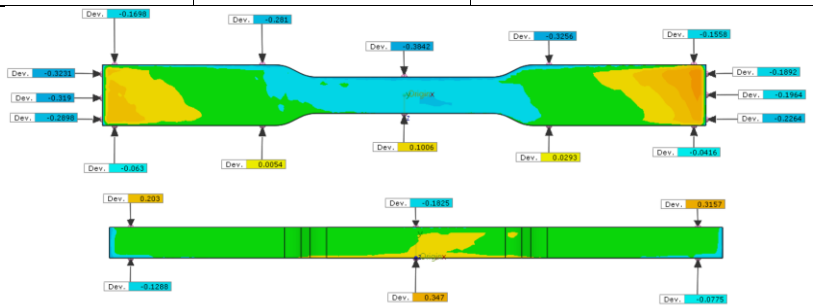
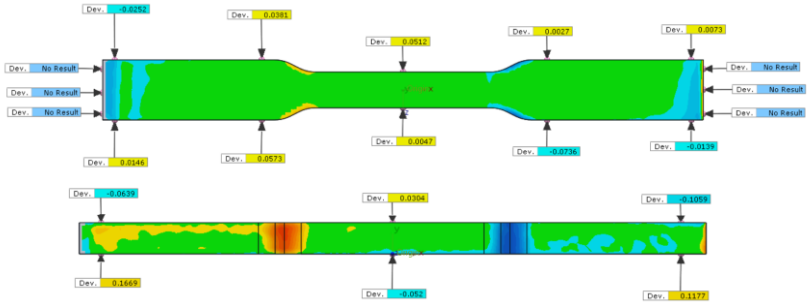
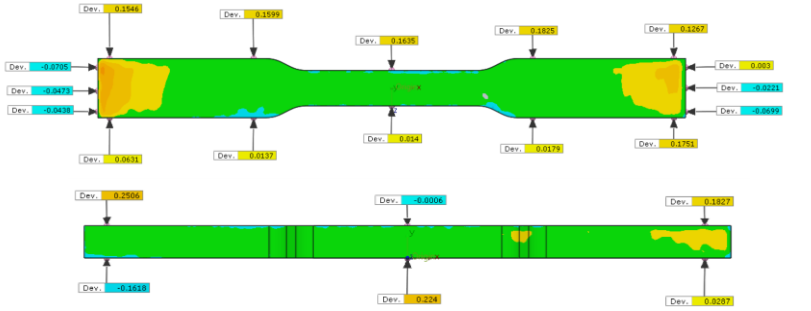
[19] C. Afteni, V. Paunoiu, M. Afteni, and V. Teodor, "Using 3D scanning in assessing the dimensional accuracy of mechanically machined parts," *IOP Conference Series: Materials Science and Engineering*, vol. 1235, no. 1, p. 012071, 2022, doi: 10.1088/1757-899x/1235/1/012071.

[20] D. Wang, L. Gao, J. Zheng, J. Xi, and J. Zhong, "Automated recognition and rebar dimensional assessment of prefabricated bridge components from low-cost 3D laser scanner," *Measurement: Journal of the International Measurement Confederation*, vol. 242, no. PA, p. 115765, 2025, doi: 10.1016/j.measurement.2024.115765.

[21] S. O'Toole, C. Osnes, D. Bartlett, and A. Keeling, "Investigation into the accuracy and measurement methods of sequential 3D dental scan alignment," *Dental Materials*, vol. 35, no. 3, pp. 495–500, 2019, doi: 10.1016/j.dental.2019.01.012.

Appendix 1. Deviation value in each point and color map

Strategy	Specimen number	Min. Deviation (mm)	Max. Deviation (mm)
A	1	**-0.3642**	0.4287
			
	2	-0.4134	0.4759
			
	3	-0.4208	0.5049
			
B	1	-0.3406	0.8388
			
	2	-0.4627	0.1999
			

Strategy	Specimen number	Min. Deviation (mm)	Max. Deviation (mm)
	3	-0.3842	0.347
			
C	1	-0.0139	0.1669
			
	2	-0.0223	0.2506
			
	3	-0.3108	0.1463
	